sciendo

Polish Journal of Chemical Technology, 20, 3, 15—19, 10.2478/pjct-2018-0033

Preparation and Up-conversion Luminescence of Yb^{3+}/Er^{3+}/GZO Ceramics

Guomin Li[1], Bing Wang[2], Rui Wang[1*], Huiling Liu[3]

[1]*School of Chemistry and Chemical Engineering, Harbin Institute of Technology, Harbin 150001, China*
[2]*College of chemical engineering, Northeast Electric Power University, Jilin 132012, China*
[3]*Harbin Institute of Technology, State Key Laboratory of Urban Water Resources and Environment, Harbin 150090, China*
[*]*Corresponding author: e-mail: wangrui001@hit.edu.cn*

Yb^{3+}/Er^{3+}/GZO ceramics have been synthesized with high temperature solid-state method. The phase and structure of the Yb^{3+}/Er^{3+}/GZO ceramics were characterized by X-ray diffraction (XRD). The XRD pattern that following ions Yb^{3+}, Er^{3+} and Ga^{3+} were well doped into the ZnO lattice. Efficient visible up-conversion (UC) red and green emission were observed under 980 nm excitation. The mechanism of the UC luminescence is investigated on the basis of the UC luminescence emission spectra, the power curve and energy level diagram. The influence of doping ions to the intensity ratio of red to green is analyzed and high purity of red light (red/green = 29.9) is finally obtained.

Keywords: Up-conversion, Yb^{3+}/Er^{3+}/GZO, Ceramics, High purity, Luminescence.

INTRODUCTION

The up-conversion (UC) is a process that can convert the photons with low energy into high energy anti-Stokes luminescence, similar to converting the near-infrared (NIR) range into the ultraviolet, visible ranges by sequential absorptions of multiple photons[1]. Due to the long lifetime excited states, superb chemical durability and abundant energy levels of the trivalent lanthanide ions, inorganic materials which embedded by the lanthanide ions are named UC materials[2–4]. The UC materials have been obtained remarkable attention on account of the unique optical and electrical properties as well as the potential applications in sensors[5], food safety[6], photocatalysis[7], photovoltaics[8, 9], biological imaging[10, 11] and therapy[12–14]. In recent years, the UC phosphors have great applied value in some domains, such as lighting, detection, and catalysis, many science researchers focused their attention on the synthesis and designs.

Because of the requisite of three primary colors (blue, green, red) emission and the adjustable relative intensities in the display, UC materials have been synthesized and widely studied recently. In UC materials, due to the fact that the host matrix is the determinant for the crystal fields around lanthanide ions, its properties can markedly influence the UC process[15]. The oxide matrix has been widely studied as the host matrix for its chemical and physical stability, high mechanical strength and environment friendly. The hexagonal wurtzite zinc oxide has caused the extensive worldwide concern and has been identified as a superduper host matrix for visible and infrared UC phosphor on account of its wide band gap, long-term stability, relatively low material cost, large exciton binding energy (60 me V) and non-toxicity[16–18]. Owning to the similar ions radius of Ga (0.62Å) and Zn (0.74Å), Ga is deemed to be one of the most effective among various choices of dopants[19]. Thereby, Ga doped ZnO (GZO) is often viewed as promising materials and numerous applications have been extensively researched[20].

Erbium ion is a very commonly researched lanthanide dopant in the domain of UC materials on account of the favorable energy level structures. Because of this character of the Er^{3+} ion, it is relatively easy to be excited by the light source of 980 nm[21]. Nevertheless, Er^{3+} ion has a relatively small absorption cross-section(ACS) at 980nm leads to a quite low pump efficiency. Enormous studies indicated that the ACS at 980 nm of Yb^{3+} ion is almost ten times larger than Er^{3+} ion[22], hence, one way to improve the UC luminescence efficiency is co-doping with Yb^{3+}, Er^{3+}. In the system of co-doped Yb^{3+}/ Er^{3+}, the sensitizer Yb^{3+} ion delivers energy to neighboring Er^{3+} which significantly enhances the intensities of the UC emission[23, 24]. As far as I know, there is almost no report on UC luminescence for the Yb^{3+}/ Er^{3+}/GZO ceramics multi-doped system. The Yb^{3+} and Er^{3+} co-doped with GZO ceramics will have been investigated necessarily in display materials and laser materials for the communication equipment to be miniaturization and integration.

In this paper, a series of Yb^{3+}/ Er^{3+}/ Ga^{3+} tri-doped ZnO ceramics have been well synthesized with the high temperature solid-state (HTSS) method. The remarkable UC emission was observed and the mechanism of the luminescence was analyzed. The influences of Yb^{3+}, Er^{3+}, Ga^{3+} on the UC luminous performance were investigated.

MATERIAL AND METHODS

$Yb^{3+}/Er^{3+}/Ga^{3+}$ tri-doped ZnO ceramic samples were synthesized via HTSS method. The raw and processed materials of the as-prepared samples were ZnO (2N purity), Ga_2O_3 (4N purity), Yb_2O_3 (4N purity) and Er_2O_3 (4N purity).

The powders were accurately weighed and sufficiently grounded enough fine in an agate mortar more than 4 hours. Subsequently, the well homogeneous powders were pressed to tablets at 16 MPa. After that, the pieces were sintered at 750°C for 2 hours and then at 1200°C for 8 hours to generate Yb^{3+}/Er^{3+}/GZO ceramics in Al_2O_3 crucible.

The orthogonal experimental design of Yb^{3+}/Er^{3+}/GZO ceramics was investigated to search the optimal doping concentrations in order to obtain the optimal UC emission. From the orthogonal experimental design, the optimizing concentrations of Ga^{3+} and Yb^{3+} can be confirmed (Table S1, Table S2, Table S3 and Fig. S1), but the concentration of Er^{3+} ought to be properly adjusted in order to obtain the superior emission under 980 nm

excitation. The concentrations of Ga^{3+} and Yb^{3+} remain invariant at 4.00 mol% and 3 mol%, respectively. The ceramic sample with concentrations (mol %) of 4.00 Ga^{3+}/3.00 Yb^{3+}/2.50 Er^{3+} is used as the reference. The proportion (mol %) of used material in prepared samples is shown in Table 1.

Table 1. Raw material compositions (mol%) of samples

Samples	Ga^{3+}[mol %]	Yb^{3+} [mol %]	Er^{3+} [mol %]
1#	4	3	2.5
2#	4	3	4
3#	4	3	5
4#	4	3	6
5#	4	3	7
6#	4	3	8

The X-ray diffraction (XRD) was detected by an XRD-6000 diffraction with the CuKα1 radiation source (λ = 0.154056 nm) to identify the crystal phase of Yb^{3+}/Er^{3+}/GZO ceramics. The UC luminescence properties were measured by an SPEX1000M spectrometer. All these measurements in this article were performed at ambient pressure and room temperature, keeping the same test condition.

RESULTS AND DISCUSSION

As shown in Fig. 1, obviously, the XRD image reveals that the diffraction peaks were completely consistent with the hexagonal wurtzite ZnO (PDF#36-1451) and no new diffraction peaks in ZnO cearmic were observed with the Yb^{3+}, Er^{3+}, Ga^{3+} doped, which demonstrating all the ions were successfully incorporated into the host matrix. The angel of all the diffraction peaks has nothing shifted with the mixing of Yb^{3+}, Er^{3+} and Ga^{3+} ions. The ion radius of erbium, ytterbium and galium is 0.88, 0.858 and 0.62Å respectively. It can be explained that although the radius of erbium ion and ytterbium ion is larger than zinc ion (0.74 Å), the gallium ion is smaller. Hence, the lattice parameter of ZnO almost has not changed during the doping process. The results suggest that the structures of the samples are not influenced changed by the doping ions, and the Yb^{3+}/Er^{3+}/GZO ceramics are still the hexagonal system. Thus, the impurity ions should replace former Zn-site, but not the interstitial sites.

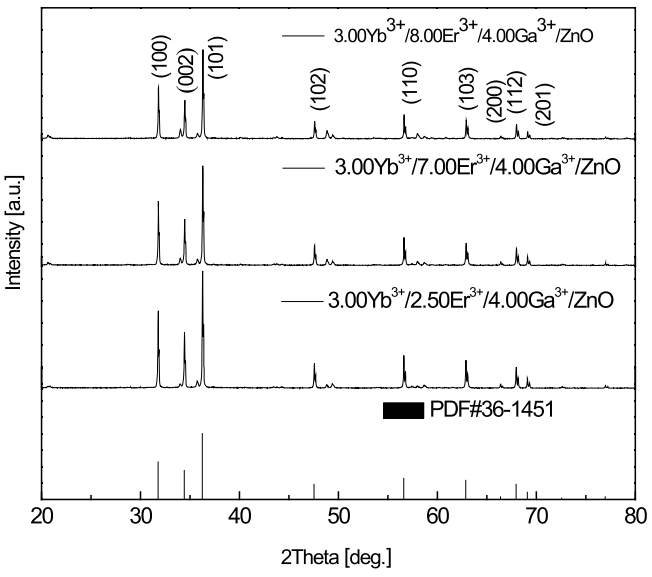

Figure 1. XRD patterns of 3.00Yb^{3+}/2.00Er^{3+}/4.00Ga^{3+}/ZnO ceramics

Figure 2 shows the UC luminescence spectrums of samples under 980 nm excitation. The spectra consist of three dominant emission regions: (i) the extremely weak green emission between 545 nm and 558 nm which is assigned to the $2_{H_{11/2}} \rightarrow 4_{I_{15/2}}$transitions of Er^{3+} ions. (ii) the slightly stronger green emission between 558 and 569 nm, attributed to the Er^{3+} ions' $4_{S_{3/2}} \rightarrow 4_{I_{15/2}}$ transitions.(iii) the intense red emission between 640nm and 695 nm corresponds to the $4_{F_{9/2}} \rightarrow 4_{I_{15/2}}$ transitions of Er^{3+} ions[25]. The red luminescence intensity is obviously strong, but the green luminescence is relatively weaker. This phenomenon is probably attributed to the comparatively higher dosage concentration of Yb^{3+} ions[26]. Thus, we focus on the increase of the dominant red emission. From Fig. 2, the red intensity is invariably increasing before the concentration of Er^{3+} reaching to 7.00 mol% and then the intensity is decreasing with the increase of Er^{3+}. This is due to the increase of the Er^{3+} ion from 2.5 mol% to 7 mol% that leads to the decrease of the distance between the adjacent Yb^{3+} ion and Er^{3+} ion, hence, the energy transfer (ET) becomes more efficient. When the quantity of the Er^{3+} ion is more than 7 mol%, the energy back transfer (EBT) from the $^4F_{9/2}$ state of Er^{3+} to $^2F_{5/2}$ state of Yb^{3+} has dominated. Therefore, the EBT leads to the decrement of the red intensity. It is worthwhile to mention that the red intensity is considerably strong, which means that Yb^{3+}/Er^{3+}/GZO ceramics are an excellent UC material. It should be very helpful

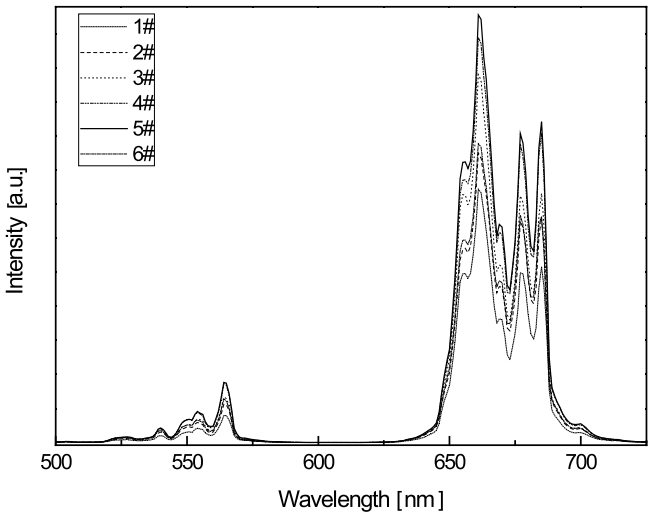

Figure 2. UC emission spectra of Yb^{3+}/Er^{3+}/GZO ceramics under 980 nm excitation. (1#:3.00Yb^{3+}/2.50Er^{3+}/4.00Ga^{3+}/ZnO; 2#:3.00Yb^{3+}/4.00Er^{3+}/4.00Ga^{3+}/ZnO; 3#:3.00Yb^{3+}/5.00Er^{3+}/4.00Ga^{3+}/ZnO; 4#:3.00Yb^{3+}/6.00Er^{3+}/4.00Ga^{3+}/ZnO; 5#:3.00Yb^{3+}/7.00Er^{3+}/4.00Ga^{3+}/ZnO; 6#:3.00Yb^{3+}/8.00Er^{3+}/4.00Ga^{3+}/ZnO)

for obtaining the novel UC phosphor which has strong emission intensity.

Figure 3 shows the decay curves of $^4F_{9/2} \rightarrow {}^4I_{15/2}(Er^{3+})$ in sample 1#, 3#, 5# and 6# at room temperature. The luminescent lifetimes of $^4F_{9/2}$ state (Er^{3+}) are 132.90μs, 134.80 μs, 137.20 μs and 136.60 μs for samples 1#, 3#, 5# and 6#, respectively. Obviously, the lifetimes of $^4F_{9/2}$

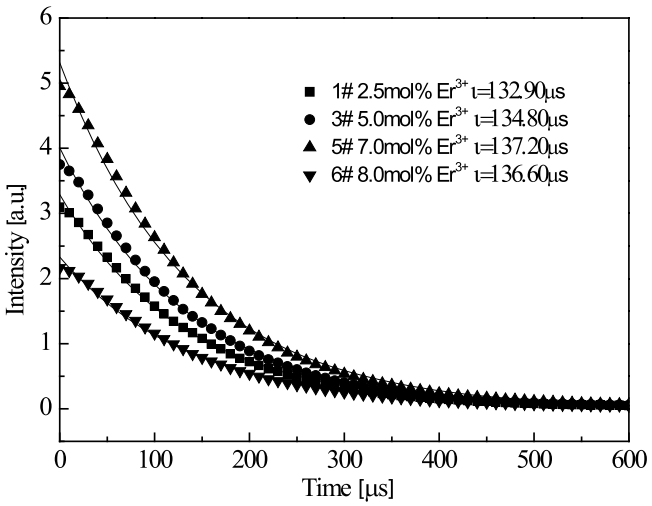

Figure 3. The decay curves of $^4F_{9/2} \rightarrow {}^4I_{15/2}(Er^{3+})$ in samples 1#, 3#, 5# and 6#

state (Er^{3+}) follows the function: $I_{(T)} = I_i + Ae^{-T/\tau}$, where I_i is background light intensity, τ is the luminescent lifetimes of red UC emission, and A is the weight factors. It can be seen that with the addition of Er^{3+}, the luminescent lifetimes of $^4F_{9/2}$ state increase first and then decrease. This is due to that with the increasing doping ratio of Er^{3+}, the ET incidence from Yb^{3+} to Er^{3+} tends to be high so that the luminescent lifetimes increase first. But the energy back transfers (EBT) from Er^{3+} to Yb^{3+} have dominated if the concentration of Er^{3+} is redundant, which reduces the luminescent lifetime of $^4F_{9/2}$ state (Er^{3+}). These results fit perfectly with the phenomenon of Fig. 2.

For the purpose of investigating the UC mechanism better, the intensity of red emission and green emission is measured with the adjustment of pump power (P). The pump power dependences of red and green emission in Yb^{3+}/Er^{3+}/GZO ceramics are shown in Fig. 4. It is well-known that UC is similar to the "unsaturated" process when being at low excitation intensity. The amount of photons can be determined by the mathematic relation $I_f \propto P^n$ when being in the emitting state[2], where I_f is luminescent intensity; n refers to laser photons that are needed to generate red or green light. The value of n can be obtained by log-log plot. Some former studies indicated that because of the "saturated" of the UC emission processes, the power dependence of UC emission turned into linear (n =1) if the excitation intensity is very high[27].

As is illustrated in Fig. 4, the slopes n of red luminescence are 1.66, 1.57, 1.61 and that of green are 1.60, 1.50, 1.53 for samples 3#, 5# and 6#, respectively. It's known that the typical red and green emission luminescence is two-photon processes at 980 nm excitation. However, it is to be noted that the slope of red and green with the typical values has a big gap. This can be explained by the "saturated" phenomenon that the competition between linear attenuation and UC could result in the depletion of intermediate excited states[28].

The UC emission processes can be inferred from Fig. 4 and Fig. 5. The schematics of energy levels, populating and UC emissions processes are shown in Fig. 5. As sensitizer, Yb^{3+} ion can be easily excited by excitation light source from $^2F_{7/2}$ level to excited $^2F_{5/2}$ level after

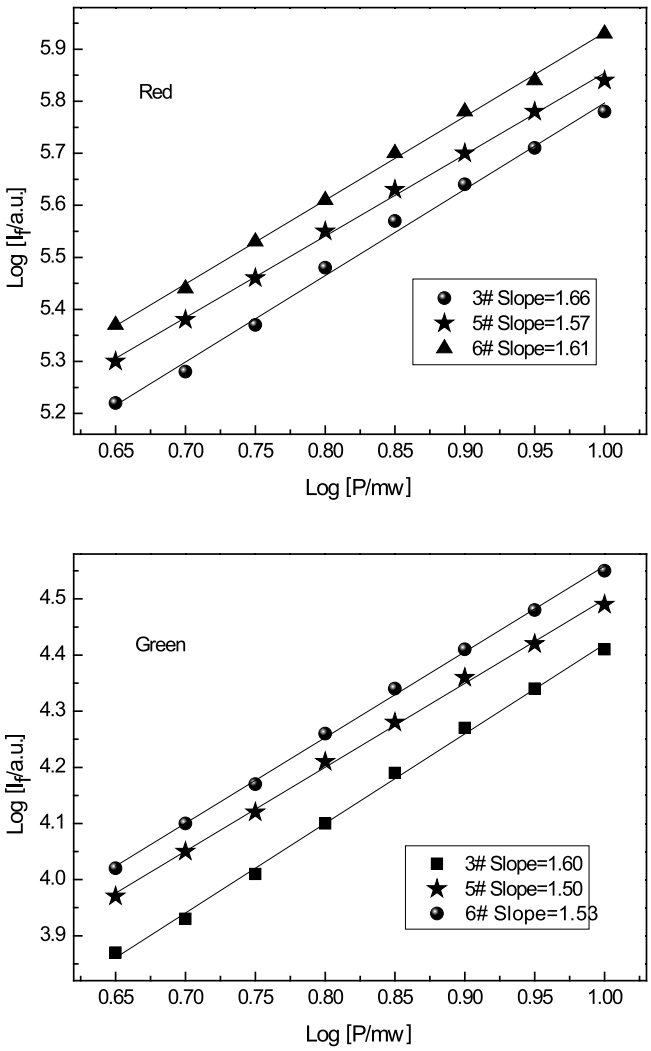

Figure 4. Pump power dependences of the green and red UC emission in Yb^{3+}/Er^{3+}/GZO ceramics

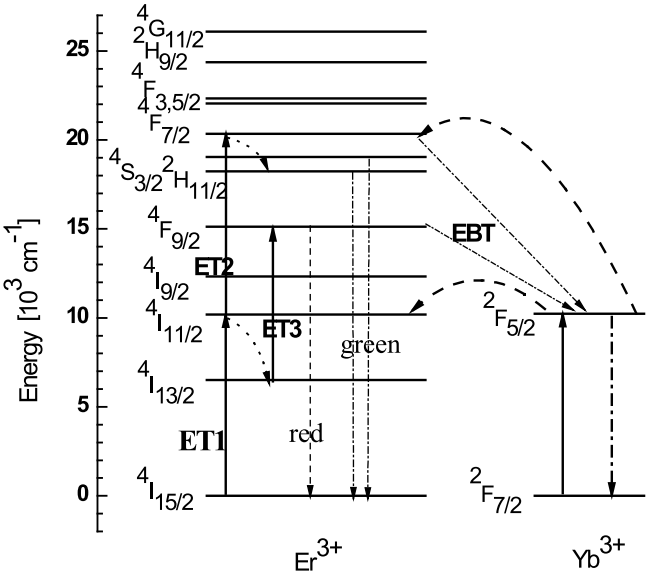

Figure 5. Energy level diagram and UC mechanism for Yb^{3+}/Er^{3+}/GZO ceramics

absorbing one laser photon. Then Yb^{3+} delivers energy to the nearby Er^{3+} ion, from which the Er^{3+} jumps to $^4I_{11/2}$ state, meanwhile, Yb^{3+} ion lost energy and decay back to $^2F_{7/2}$ state. Afterwards, the excited state Er^{3+} ion is pumped by the same laser from $^4I_{11/2}$ state to $^4F_{7/2}$ state via ET process. Alternatively, the energy transfer process

$^4I_{11/2}Er^{3+} + {}^4I_{11/2}Er^{3+} \rightarrow {}^4I_{15/2}Er^{3+} + {}^4F_{7/2}Er^{3+}$ or the excited state absorption (ESA) process $^4I_{11/2}Er^{3+} + hv \rightarrow {}^4F_{7/2}Er^{3+}$ can also populate the $^4F_{7/2}$ state. Subsequently, the electrons at $^4F_{7/2}$ state quickly drop to $^4S_{3/2}$ or $^2H_{11/2}$ levels by nonradiative transition. Afterwards, the green emission occurs by radiative decay. A portion of the electrons at $^4F_{7/2}$ level can get to the lower $^4F_{9/2}$ state by non-radiatively decay and generate red emission. Another approach to populate the $^4F_{9/2}$ state is that the Er^{3+} at intermediate $^4I_{11/2}$ level non-radiatively decay to $^4I_{13/2}$ state, subsequently, the electron at $^4I_{13/2}$ state is excited to $^4F_{9/2}$ level by means of ESA or ET.

The results of the orthogonal experimental show that with the addition of Ga^{3+} or Yb^{3+} ions, the intensity of red to green light ratio (RGR) is obviously increasing. When the component is 4 mol% Ga^{3+}/4mol% Yb^{3+}/1.5mol% Er^{3+}, the RGR is even to 29.9 and obtains a high purity of red light. But it should be pointed out that with the increasing doping ratio of Er^{3+} ion, the RGR is decreasing as shown in Fig. 6. It may be explained by the fact that the cross-relaxation (CR) process $^4I_{11/2}Er^{3+} + {}^4I_{11/2}Er^{3+} \rightarrow {}^4I_{15/2}Er^{3+} + {}^4F_{7/2}Er^{3+}$ occurs with the increase of the Er^{3+} ion, inducing an increment of the population on $^4F_{7/2}$ state. In the meanwhile, the existence of the CR process causes a decrement of the population on the $^4I_{11/2}$ state and leads to the reducing of the non-radiative decay to $^4I_{13/2}$ state . Therefore, with the increasing of the Er^{3+} ion, the green emission's intensity increases faster than the red one and results in the diminution of the RGR. The finding reveals that rational controlling the concentration of doping ions can obtain a variable proportion of red to green, even the high purity of red light.

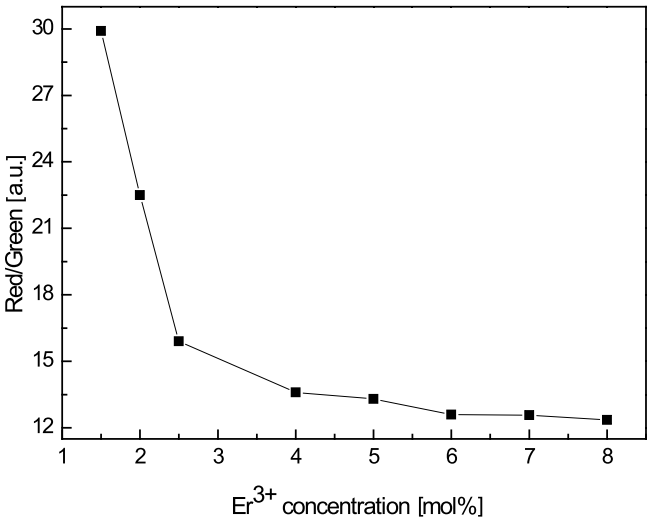

Figure 6. The intensity ratio of red to green in Yb^{3+}/Er^{3+}/GZO ceramics

CONCLUSIONS

In summary, the Yb^{3+}/Er^{3+} co-doped GZO ceramics were triumphantly fabricated by HTSS method, the efficient UC emission was recorded. XRD patterns indicated that doping ions replaced the normal Zn-site and do not change the crystal structure of Yb^{3+}/Er^{3+}/ GZO. The pump dependence and UC mechanism show that the UC red and green emission are two-photon processes under 980nm excitation and assigned to $^4F_{9/2} \rightarrow {}^4I_{15/2}$ and $^2H_{11/2}, {}^4S_{3/2} \rightarrow {}^4I_{15/2}$. The results reveal that rational controlling the concentration of doping ions can obtain a variable proportion of red to green even the red light is high purity. The decay curves demonstrated that if the concentration of Er^{3+} ions is redundant, the EBT will occur and lead the intensity of UC emission to decrease. The experimental results show that the GZO is one of the potential UC host materials.

ACKNOWLEDGEMENTS

This work was supported by the NSF of China (11374080).

LITERATURE CITED

1. Auzel, F. (2004). Upconversion and anti-stokes processes with f and d ions in solids. *Chem. Rev.* 104(1), 139–174. DOI: 10.1021/cr020357g.

2. Chen, G., Qiu, H., Prasad, P. N. & Chen, X. (2014). Upconversion nanoparticles: design, nanochemistry, and applications in theranostics. *Chem. Rev*. 114(10), 5161–5214. DOI: 10.1021/cr400425h.

3. Yan, S.Q. (2015). Synthesis and luminescence of $BiPO_4$:Tb^{3+} nanowires by a hydrothermal process. Mater. Manuf. Process. 30, 591–594. DOI: 10.1080/10426914.2014.994777.

4. Liu, Z.L., Zhou, H.Y., Du, L.P. & Yang, H. (2012). Synthesis and luminescence properties of Y_2O_3:Tb^{3+}, Dy^{3+}. Mater. Manuf. Process. 27 (12), 1306–1309. DOI: 10.1080/10426914.2012.663146.

5. Camargo, A.S.S., Possatto, J.F., Nunes, L.A.D.O., Botero, É.R., Andreeta, É.R.M., Garcia, D. & Eiras, J.A. (2006). Infrared to visible frequency upconversion temperature sensor based on Er^{3+}-doped PLZT transparent ceramics. Solid State Commun. 137(1–2), 1–5. DOI: 10.1016/j.ssc.2005.10.020.

6. Pan, W., Zhao, J. & Chen, Q. (2015). Fabricating upconversion fluorescent probes for rapidly sensing foodborne pathogens. *J. Agric. Food Chem.* 63 (36), 8068–8074. DOI: 10.1021/acs.jafc.5b02331.

7. Reszczyńska, J., Grzyb, T., Sobczak, J.W., Lisowski, W., Gazda, M., Ohtani, B. & Zaleska, A. (2015). Visible light activity of rare earth metal doped (Er^{3+}, Yb^{3+} or Er^{3+}/Yb^{3+}) titania photocatalysts. Appl. Catal. B 163, 40–49. DOI: 10.1016/j.apcatb.2014.07.010.

8. Rony, S.K., Jörg, B., Jordan, A.H., Alexandre, H, Fan, D., Felix, N.C. (2012). Upconversion-powered photoelectrochemistry. Rsc Adv. 48, 209–211. DOI: 10.1039/c1cc16015j.

9. Martín-Rodríguez, R., Fischer, S., Ivaturi, A., Froehlich, B., Krämer, K.W., Goldschmidt, J.C., Richards, B.S. & Meijerink, A. (2013). Highly efficient IR to NIR upconversion in Gd_2O_2S: Er^{3+} for photovoltaic applications. *Chem. Mater.* 25(9), 1912–1921. DOI: 10.1021/cm4005745.

10. Yao, C., Wang, P., Zhou, L., Wang, R., Li, X., Zhao, D. & Zhang, F. (2014). Highly biocompatible zwitterionic phospholipids coated upconversion nanoparticles for efficient bioimaging. *Anal. Chem*. 86(19), 9749–9757. DOI: 10.1021/ac5023259.

11. Wu, X., Chen, G., Shen, J., Li, Z., Zhang, Y. & Han, G. (2015). Upconversion nanoparticles: a versatile solution to multiscale biological imaging. Bioconjugate Chem. 26(2), 166–175. DOI: 10.1021/bc5003967.

12. Li, W., Wang, J., Ren, J. & Qu, X. (2014). Near-infrared upconversion controls photocaged cell adhesion. J. Am. Chem. Soc. 136(6), 2248–2251. DOI: 10.1021/ja412364m.

13. Dou, Q., Idris, N.M. & Zhang, Y. (2013). Sandwich--structured upconversion nanoparticles with tunable color for multiplexed cell labeling. Biomater. 34(6), 1722–1731. DOI: 10.1016/j.biomaterials.2012.11.011.

14. Wang, Z., Li, X., Song, Y., Li, L., Shi, W. & Ma, H. (2015). An upconversion luminescence nanoprobe for the ultrasensitive detection of hyaluronidase. *Anal. Chem.* 87 (11), 5816–5823. DOI: 10.1021/acs.analchem.5b01131.

15. Liu, Z., He, T. & Xue, Q. (2016). Synthesis and up-conversion emission of β-Ca_2SiO_4 :(Er^{3+}, Yb^{3+}). Mater. Manuf. Process. 31(2), 194–197. DOI: 10.1080/10426914.2015.1048366.

16. Surabi, M.A., Chandradass, J. & Park, S. (2015). ZnO--based thin film transistor fabricated using radio frequency magnetron sputtering at low temperature. Mater. Manuf. Process. 30, 175–178. DOI: 10.1080/10426914.2014.892973.

17. Jang, Y.R., Yoo, K.H., Ahn, J.S., Kim, C. & Park, S.M. (2011). 1.54μm emission mechanism of Er-doped zinc oxide thin films. *Appl. Surf. Sci.* 257(7), 2822–2824. DOI: 10.1016/j.apsusc.2010.10.069.

18. Vijayalakshmi, U., Chellappa, M., Anjaneyulu, U., Manivasagam, G. & Sethu, S. (2016). Influence of coating parameter and sintering atmosphere on the corrosion resistance behavior of electrophoretically deposited composite coatings. Mater. Manuf. Process. 31, 95–106. DOI: 10.1080/10426914.2015.1070424.

19. Chawalit, B., Sanpet, N., Sutthipoj, S., Pipat, R.,Supab, C. & Duangmanee, W. (2015). Effect of gallium interlayer in ZnO and Al-doped ZnO thin films. Integr. Ferroelectr. 165, 121–130. DOI: 10.1080/10584587.2015.1063914.

20. Ng, Z., Chan, K., Low, C., Kamaruddin, S.A. & Sahdan, M.Z. (2015). Al and Ga doped ZnO films prepared by a sol--gel spin coating technique. Ceram. Int. 41, S254–S258. DOI: 10.1016/j.ceramint.2015.03.183.

21. Hao, S., Sun, L., Chen, G., Qiu, H., Xu, C., Soitah, T.N., Sun, Y. & Yang, C. (2012). Synthesis of monoclinic Na_3ScF_6:1mol% Er^{3+}/2mol% Yb^{3+} microcrystals by a facile hydrothermal approach. *J. Alloys Compd*. 522, 74–77. DOI: 10.1016/j.jallcom.2012.01.080.

22. Meng, X., Liu, C., Wu, F. & Li, J. (2011). Strong up-conversion emissions in ZnO:Er^{3+}, ZnO:Er^{3+}-Yb^{3+} nanoparticles and their surface modified counterparts. *J. Colloid Interface Sci*. 358(2), 334–337. DOI: 10.1016/j.jcis.2011.03.036.

23. Tamrakar, R.K., Bisen, D.P., Upadhyay, K. & Sahu, I.P. (2015). Comparative study and role of Er^{3+} and Yb^{3+} concentrations on upconversion process of Gd_2O_3:Er^{3+} Yb^{3+} phosphors prepared by solid-state reaction and combustion method. *J. Phys. Chem.* C 119(36), 21072–21086. DOI: 10.1021/acs.jpcc.5b06443.

24. Chen, G.X., Ding, C.J., Wu, E., Wu, B.T., Chen, P., Ci, X.T., Liu, Y., Qiu, J.R., Zeng, H.P. (2015). Tip-enhanced upconversion luminescence in Yb^{3+}-Er^{3+} codoped $NaYF_4$ nanocrystals. *J. Phys. Chem. C* 119(39), 22604–22610. DOI: 10.1021/acs.jpcc.5b04387.

25. Lu, D., Cho, S.K., Ahn, S., Brun, L., Summers, C.J., Park, W. (2014). Plasmon enhancement chanism for the upconversion processes in $NaYF_4$:Yb^{3+}, Er^{3+} nanoparticles: axwellversus förster. ACS Nano 8(8), 7780–7792. DOI: 10.1021/nn5011254.

26. Bai, Y., Wang, Y., Yang, K., Zhang, X., Song, Y., & Wang, C.H. (2008). Enhanced upconverted photoluminescence in Er^{3+}, and Yb^{3+}, codoped ZnO nanocrystals with and without li^{+}, ions. Optics Communications, 281(21), 5448–5452. DOI: 10.1016/j.optcom.2008.07.041.

27. Li, D., Dong, B., Bai, X., Wang, Y. & Song, H. (2010). Influence of the TGA modification on upconversion luminescence of hexagonal-phase $NaYF_4$:Yb^{3+}, Er^{3+} nanoparticles. J. Phys. Chem. C 114(18), 8219–8226. DOI: 10.1021/jp100893k.

28. Gilliland, G.D., Powell, R.C. & Esterowitz, L. (1988). Spectral and up-conversion dynamics and their relationship to the laser properties of $BaYb_2F_8$:Ho^{3+}. Physical Review B. DOI: 10.1103/PhysRevB.38.9958.